GENERAL ELECTRIC

ENERGY SYSTEMS AND TECHNOLOGY DIVISION

GENERAL ELECTRIC COMPANY . . ENERGY SYSTEMS PROGRAMS DEPARTMENT
1 RIVER ROAD, SCHENECTADY, NEW YORK 12345
Building 2 - Room 439
(518) 385-8924

MASTER

February 27, 1981

U.S. Department of Energy
Patent Group
P.O. Box E
Oak Ridge, Tennessee 37830

Attention: Cognizant DOE Patent Counsel

Subject: Contract No. DE-AC01-80ET17091
Request for Patent Clearance

Gentlemen:

Forwarded herewith is a paper entitled "High Performance Cyclone Development". Said paper is to be presented at the Third Symposium on the Transfer and Utilization of Particulate Control Technology to be held in Orlando, Florida, March 9-12, 1981.

Subject paper has been reviewed for possible inventive subject matter and no inventions or discoveries are deemed to be disclosed.

Your prompt review and telephone clearance by Friday, March 6, 1981 would be greatly appreciated.

Very truly yours,

Don Luce

DH Luce, Supervisor
Contract Administration

DHL/kt
Enclosure

APPROVED FOR RELEASE OR PUBLICATION - O.R. PATENT GROUP
BY SDH DATE 3/4/81

DISCLAIMER

CONF-810319--1

HIGH PERFORMANCE CYCLONE DEVELOPMENT

W.B. Giles
Corporate Research and Development
General Electric Company
Schenectady, New York

Abstract

The results of cold flow experiments at atmospheric conditions of an air-shielded 18 inch diameter electrocyclone with a central cusped electrode are reported using fine test dusts of both fly-ash and nickel powder. These results are found to confirm expectations of enhanced performance, similar to earlier work on a 12 inch diameter model.

An analysis of the combined inertial-electrostatic force field is also presented which identifies general design goals and scaling laws. From this, it is found that electrostatic enhancement will be particularly beneficial for fine dusts in large cyclones.

Recommendations for further improvement in cyclone collection efficiency are proposed.

Introduction

Earlier experiments found (1) a marked influence of natural electrostatic forces in enhancing cyclone collection efficiencies, particularly at low velocities. This naturally-occurring phenomena, if present, is evident as a relatively constant collection efficiency with throughput. Evidence of this anomolous behavior is present in the literature (2,3,4,5,6) without explanation. Also Siemens' experience found weak influence due to both velocity and cyclone size (7). Experiments using a Faraday cage to sense air-borne particle charge levels show that triboelectric charges are induced by particle-wall collisions. Certain dusts are found to have a much higher propensity for this charge generation than others. For example, Exxon flyash have been observed to generate levels of 100 fold greater than CURL flyash. Within the cyclone, these charged particles are mutually repulsive and the resultant space charge augments inertial separation. In the present work, applied electrostatics are used to enhance performance. Similar effort is found in the literature (8,9,10). One study (2), in fact, concludes that the benefit does not justify the complication. However, for hot gas cleaning in coal-fired power generation systems large cyclones offer an economically attractive option. Small, multicyclones pose a substantial risk of fouling, whereas large conventional cyclones have poor performance for fine particle collection. Thus, the objective is to attempt to obtain, in large cyclones, the equivalent performance of small, inertial cyclones through the application of electrostatics. In addition, the cyclonic action provides a mechanism of dust removal from the collecting electrode surface that precludes the problem of dust conductivity at high temperature which inhibits collection with conventional electrostatic precipitators.

Preliminary Experiment

The general characteristics of using applied electrostatics are shown in Figure 1. Here, a central cusped electrode was supported within the exhaust duct to protrude down into the cyclone body. When charged, this electrode provides an electric field from the electrode to the grounded cyclone body with a corona source at the four cusped edges of the electrode. The data indicates that the application of a charge results in a significant improvement in collection at the lower test velocities.

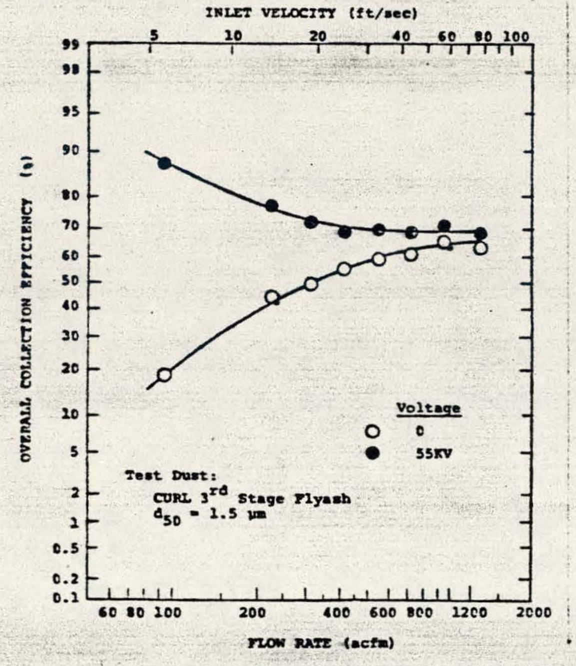

FIGURE-1 12-INCH AIR SHIELD MODEL WITH CUSPED ELECTRODE

General Theory

In a reverse flow cyclone, a swirl flow is induced, and the flow moves radially inward to the exhaust. A centrifugal, or inertia force, F_i, is produced on the air-borne particles acting against the inward drag force, F_d. Additionally, with charged particles in an electric field, an electrostatic force, F_e, aids the centrifugal force to promote particle separation.

The separative efficiency of cyclone, η, is functionally dependent on the separative parameter, S, which can be determined empirically. The general collection characteristics may be studied by considering the combined inertial-electrostatic separative parameter, S, where

$$S = \frac{F_i}{F_d}\left(1 + \frac{F_e}{F_i}\right) = S_i\left(1 + \frac{F_e}{F_i}\right) \qquad (1)$$

in which,

$$F_i = \rho_p \frac{\pi}{6} d_p^{\,3} \frac{V_t^{\,2}}{r}, F_d = 3\pi\mu d_p U_r, \quad F_e = q_p E(r)$$

and,

$$q_p = 3\pi\varepsilon_o d_p^{\,2} E_c, \text{ with } \quad E_c \approx E(r) \approx \frac{V_o}{r\,\ln(D/Del)}$$

The maximum g-field occurs* at the edge of the core flow region which is assumed here as equal to the exit duct radius or $r=D_e/2$. The maximum E-field, however, is greater at smaller radius, e.g. particles convected to smaller radius can become electrostatically dominated. For present purpose, the E-field will be evaluated also at $r=D_e/2$.

Since the radial inflow velocity is approximately uniform,

$$\pi D_e L\ U_r = \left(\frac{A_i}{D^2}\right) D^2 V_i = Q, \text{ where } A_i = 2\left(\frac{x}{D}\right)^2 D^2$$

The spin-up, via conservation of angular momentum, is

$$(1+2x')D\ V_i = D_e V_t,\ x' = x/D$$

Then equation 1 becomes

$$S = k_1 \frac{V_i}{D_e}\left[1 + \frac{k_2}{(V_i/D_e)^2}\right] \qquad (2)$$

where,

$$k_1 = \frac{\pi \rho_p d_p^{\,2}}{18\mu}\left(\frac{1+2x'}{x'}\right)^2 \frac{L}{D_e}$$

$$k_2 = \frac{\varepsilon_o}{\rho_p d_p D_e^{\,3}}\left(\frac{D_e}{D}\right)^2\left(\frac{1}{1+2x'}\right)^2\left(\frac{6\ \ V_o}{\ln D/Del}\right)^2$$

Equation 2 indicates a minimum exists when $V_i/D_e = \sqrt{k_2}$, and this minimum separative parameter is

$$S_{min} = \frac{\pi}{1.5\mu}\sqrt{\frac{\rho_p d_p^{\,3}\varepsilon_o}{D_e^{\,3}}}\ \frac{L}{D}\left(\frac{1+2x'}{x'^2}\right)\frac{V_o}{\ln D/Del} \qquad (3)$$

The design of the electrocyclone should be such as to make S_{min} as large as possible. This indicates that the desired features are:

1. Long cyclone length, L/D, consistent with vortex stability
2. Small inlet area, x', consistent with good inlet flow swirl turning, e.g. flow acceleration into the annular passage
3. Small exit diameter, D_e
4. High applied voltage, V_o, consistent with arc-over constraints, and
5. Large electrode diameter, Del, consistent with the internal corona production.

In addition, cyclone operation should be at maximum allowable velocity (subject to constraints of erosion, pressure loss and particle bouncing). This allows minimized cyclone size, D_e, to maximize performance.

*Some independent evidence suggests that in the presence of a strong corona source the E-field may be relatively constant.

The influence of electrostatic augmentation, relative to pure inertial separation, S_o, is indicated by the ratio,

$$S/S_o = 1 + \frac{\varepsilon_o D}{\rho_p d_p V_i^2} \left(\frac{D_e}{D}\right)\left(\frac{1}{1+2x'}\right)\left(\frac{6 \; V_o/D}{\ln \; D/D_{el}}\right) \qquad (4)$$

thus, there is a greater enhancement with large electrostatic cyclones, than with small cyclones.

Test Model Design

The general design configuration was derived from Stairmand's High Efficiency design with major modifications. An outline of the design is shown in Figure 2. Similarity is found in the cylindrical, conical and exhaust length-to-diameter ratios, plus use of a small inlet area ($A_i = 0.1D^2$). In addition, the air shield feature (12) is employed using a double scroll inlet with the clean air inlet sized for 80% of the total flow, and a conical section added to the exhaust inlet to increase gas spin-up.

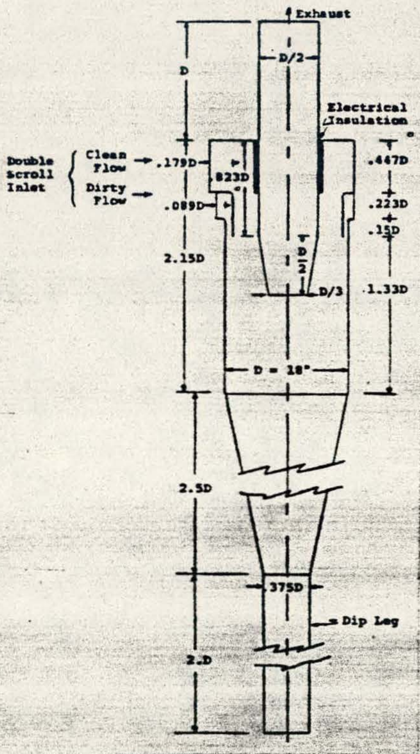

FIGURE 2: 18" D ELECTROCYCLONE MODEL

The electrostatic features included the electrical isolation of the lower end of the exhaust duct with high voltage supplied to a central electrode. The original configuration, shown in Figure 3, consisted of bundled wire and is similar to the electrode Petroll and Langhammer (2). It was found to result in excessive vibration, singing, and poor cyclone performance. The next design used a central cusped electrode supported by crossed non-conductive rod. Figure 4 shows the original installation in the 12-inch diameter air shield cyclone as used in the experiment in Figure 1. This electrode was then incorporated in the 18-inch diameter electrocyclone testing program.

The completed cold flow electrocyclone installation is shown in Figure 5.

General Experimental Technique

The experimental procedure consisted of supplying metered clean and dirty flows (80% and 20% respectively) to the two cyclone inlets. Both flows were provided by a blower using filtered air at the input to the blower. A small fluid bed dust generator, operating on shop air, provided a known particulate contaminant to the dirty air cyclone inlet line.

Particle measurement was provided by two optic techniques. One measured the overall dust concentration at both the inlet

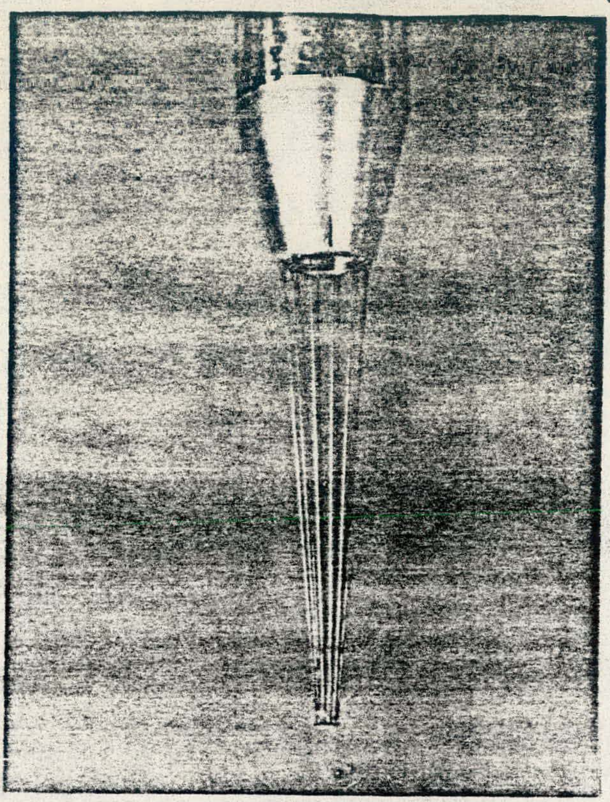

FIGURE 3: BUNDLED WIRE ELECTRODE

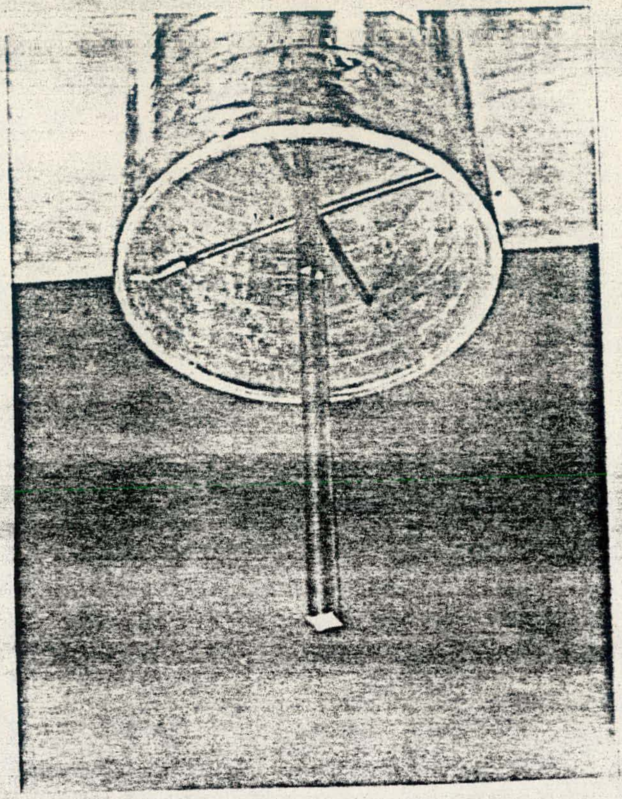

FIGURE 4: CENTRAL CUSPED ELECTRODE IN AIR SHIELD EXHAUST

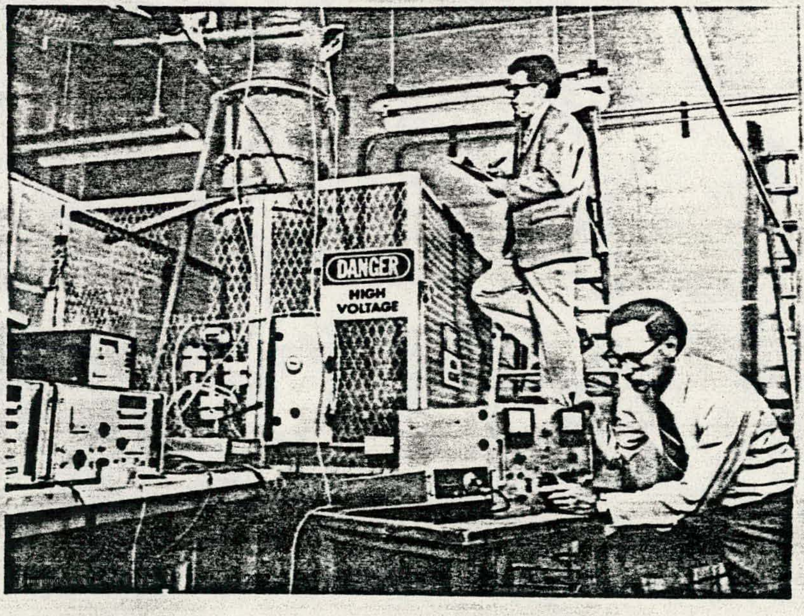

FIGURE 5: EIGHTEEN INCH DIAMETER ELECTROCYCLONE TEST INSTALLATION

and outlet using two PILLS V Mass Concentration Monitors. The other measured size distribution at both inlet and outlet using two Royco Airborne Particle Counter Systems. The latter used isokinetic probe sampling, followed by dilution to avoid coincidence errors.

Results and Discussion

Pressure Loss

The flow impedance of the cyclone was determined by measuring pressure loss, Δp, versus input volume flow. The correlation based on inlet kinetic heads to give

$$\Delta p/\frac{1}{2}\rho V_i^{\,2} = 8.2 \text{ for } D_e/D = \frac{1}{3}$$

This may be compared to the reported (11) High Efficiency Stairmand design giving a value

$$\Delta p/\frac{1}{2}\rho V_i^{\,2} = 6.0 \text{ for } D_e/D = \frac{1}{2}$$

Scoping Experiments

Preliminary experiments were first tried with an external corona particle charger, and separately, with an internal voltage field. Neither were found to yield significant enhancement. However, tests with an internal corona source to produce both particle charging and an applied voltage field did show promise as found in Figure 1. The results of a series of scoping tests using the 18 in. diameter electrocyclone are summarized in Figure 6. These results indicated that an upstream corona source was not significant and a positive corona was slightly beneficial at atmospheric conditions, relative to a negative corona source. The data shown is plotted in terms of the overall efficiency vs. volumetric flow times the square of input mass mean particle size as an indicator of the inertial similarity parameter. CURL flyash is used as the test dust and the exhaust duct is insulated from ground.

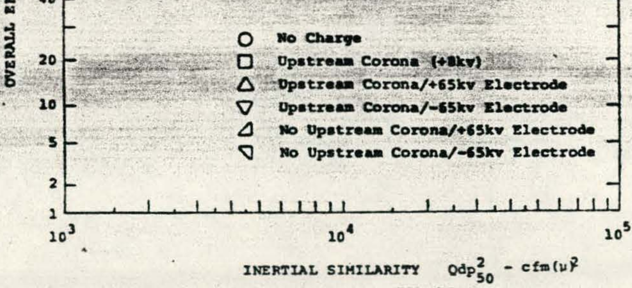

FIGURE 6: SCOPING EXPERIMENTS WITH 18" D ELECTROCYCLONE MODEL

Inertial Performance with Flyash and Nickel

Figure 7 shows the experimentally determined fractional efficiency of the electrocyclone operated in an uncharged state with flyash; and, with nickel shown in Figure 8.

Correlation with the inertial separative parameter is found to be excellant for the case of flyash. Good repeatability is noted with replicated runs. Also overall efficiency versus mass average separative parameter (solid symbols) is in good agreement with fractional efficiency data.

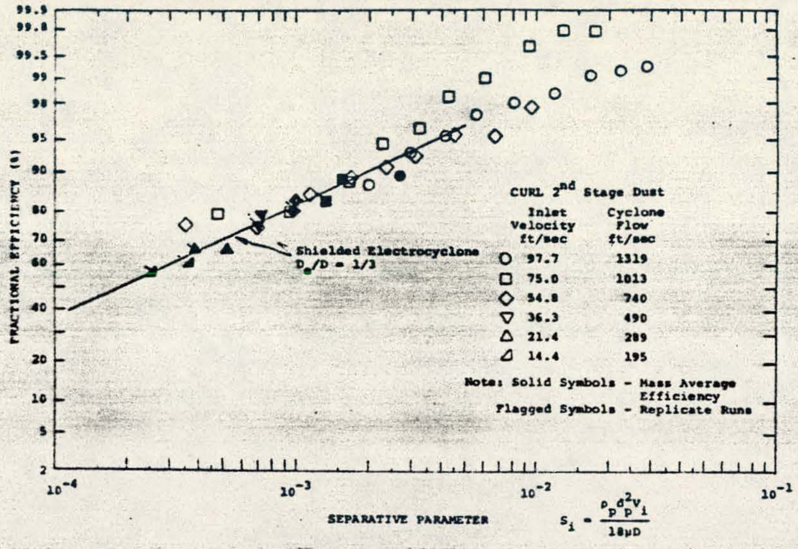

FIGURE 7: UNCHARGED ELECTROCYCLONE (18"D)

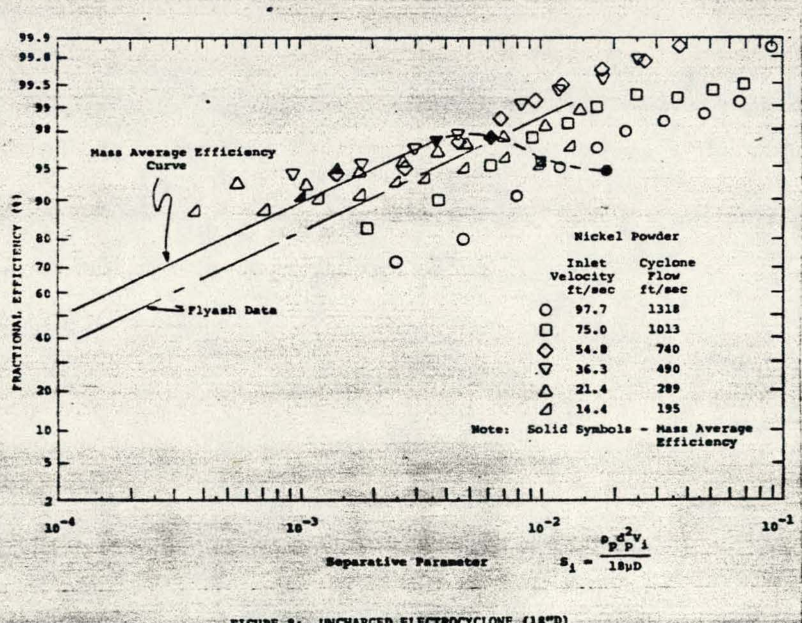

FIGURE 8: UNCHARGED ELECTROCYCLONE (18"D)

The data using nickel, in Figure 8, (with particle density taken as 8, versus 2 for flyash) shows the same approximate agreement, particularly for data in the range of 21 to 75 ft/sec inlet velocity. The mass average efficiency curve, however, is at significant variance from the fractional efficiency curves. The behavior of the former is suggestive of "coarse particle bouncing." The data suggests that this effect is primarily dependent on particle kinetics, $\rho_p V_i^2$, rather than particle size, d_p, since the effect is not evident in the fractional efficiency data. This is taken to infer that performance degradation might become important for flyash at velocities greater than 100 ft/sec; however, material differences may be expected to play an important role.

The inferred fractional efficiency is found to fit the approximate empirical expression;

$$\ln(1-\eta_f) = -1.75 \left[\frac{\rho_p d_p^{\,2} V_i}{18\mu D} 10^3\right]^{1/2} \qquad (5)$$

Electrostatic Performance

Figure 9 shows the relative influence on overall cyclone efficiency with a charged central cusped electrode. The exhaust duct was electrically insulated from ground and hence, could float at some intermediate voltage level. Typical current flux was measured at 0.35 ma. It is noted that performance is substantially independent of cyclone inlet velocity and significantly superior to inertial operation. Figure 10 shows the same data after minor correction for particle size errors, associated with the PILLS sensor versus the mass average separative parameter. Also shown are typical measurements of inlet and outlet flyash size distributions. The very close similarity of these distributions can lead to experimental errors in deducing fractional efficiency. Figure 11 shows the deduced fractional efficiency with a charged central electrode. Generally, it is found that efficiency is substantially independent of inlet velocity.

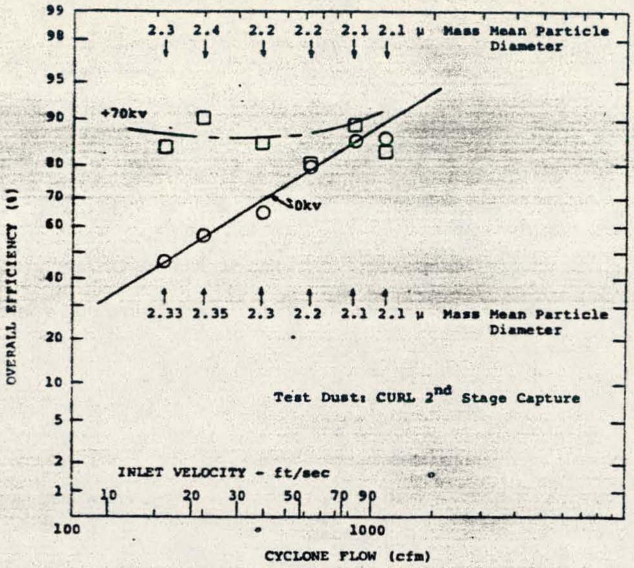

FIGURE 9: OVERALL EFFICIENCY AT 18" D ELECTROCYCLONE WITH CENTRAL CUSPED ELECTRODE AND FLOATING EXHAUST

Using nickel as a test dust, as shown in Figure 12, there is a more distinct difference between inlet and outlet dust distributions, and thus markedly less ambiguity in measuring fractional efficiency. Again, there appears to be a pronounced performance degradation due to particle kinetic energy. This is clearly evident in Figure 13 which shows the overall efficiency as measured by the PILLS instrumentation versus cyclone velocity.

Theoretical Correlation

The performance data with a charge and using flyash may be achieved by replacing the inertial term in equation 5 with the complete separative parameter, or

$$\ln(1-\eta_f) = -1.75 \left[k'_1 \frac{V_i}{D_e} \left(1+\frac{k_2 D_e^2}{v_i^2}\right) 10^3\right]^{0.5} \qquad (6)$$

where

$$k_1 = \frac{\rho_p d_p^2}{18\mu} \frac{D_e}{D}$$

An analytic fit may be taken from the experimental data at a median velocity of 40 ft/sec using η_f=0.83 at d_p=2μ and η_f = 0.935 at d_p = 4μ to give,

$$\left[\frac{\ln(1-\eta_f)}{-1.75}\right]^2 = 1.18 \times 10^{-3} \, d_p^2 \, V_i \left(1+\frac{14245.}{d_p V_i^2}\right) \qquad (7)$$

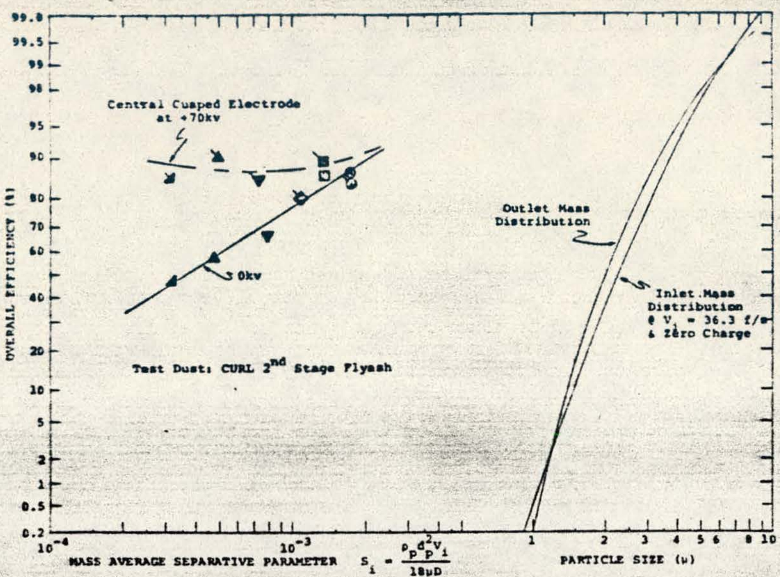

FIGURE 10: OVERALL EFFICIENCY & SAMPLE DISTRIBUTION AT 18"D ELECTROCYCLONE TEST

wherein the particle size is in microns and the cyclone inlet velocity is in ft/sec.

The trends of this theoretical correlation are shown in Figure 14 over the general range of experimentation. It is noted that a loss of performance is anticipated at increased velocity due to a weakening of the relative influence of electrostatics and the predicted performance increases with particle size. Equation 7, however, predicts a higher performance level for coarse particles than found experimentally.

The indicated enhancement for electrostatic enhancement is

$$\frac{\ln(1-\eta_f)}{\ln(1-\eta_{f_o})} = 1 + \frac{14245.}{d_p V_i^2} \approx 1 + \frac{\varepsilon_o D}{\rho_p d_p V_i^2}\ \frac{D_e}{D}\ \frac{1}{1+2x'}\ \left(\frac{2\ 6\ V_o/D_e}{\ln D/Del}\right)^2 \quad (8)$$

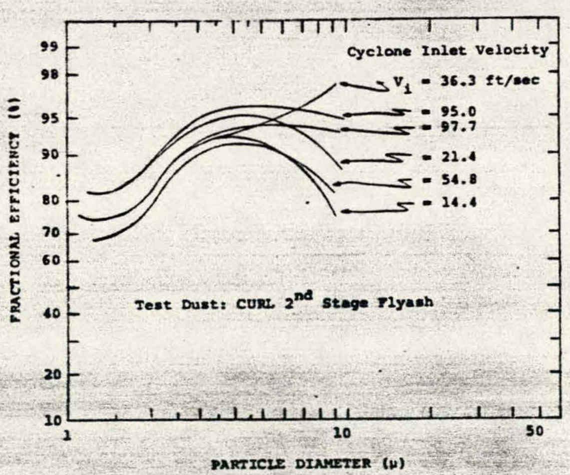

FIGURE 11: FRACTIONALLY EFFICIENCY OF ELECTROCYCLONE WITH CENTRAL CUSPED ELECTRODE AT +70kv (0.35 ma)

Thus, for a fixed voltage gradient, geometric similarity, and fixed inlet velocity, performance is improved with electrostatic augmentation at increased cyclone scale.

For application in the PFB-CFCC system, special interest is directed to controlling erosive particles of the order of 5 microns and larger. Assuming cyclone inlet velocities of the order of 100 ft/sec, the indicated enhancement in separative effectiveness (from equation 8) is increased by 28% for an 18 inch diameter cyclone, or by 112% for a 6 ft dia. cyclone. This empirically-deduced theoretical correlation finds that electrostatic augmentation should be highly desirable for turbine erosion control using large cyclones. However, the apparent variation of coarse particles is critically important.

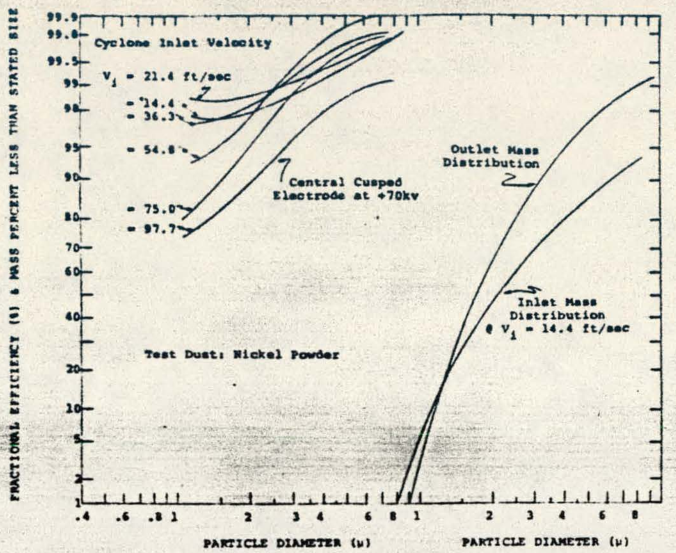

FIGURE 12: FRACTIONAL EFFICIENCY & SAMPLE DISTRIBUTION AT 18"D ELECTROCYCLONE TEST

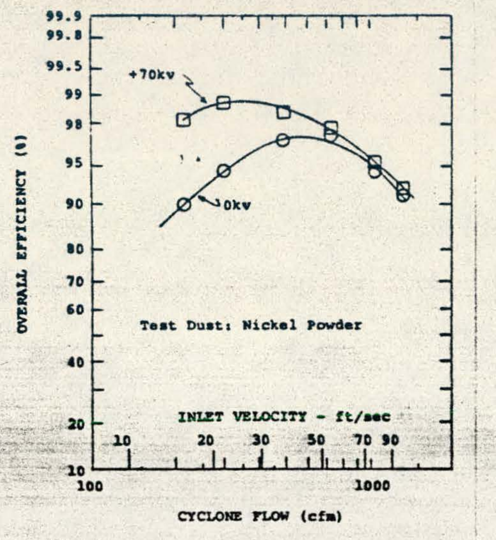

FIGURE 13: OVERALL EFFICIENCY OF ELECTROCYCLONE WITH CENTRAL CUSPED ELECTRODE & FLOATING EXHAUST

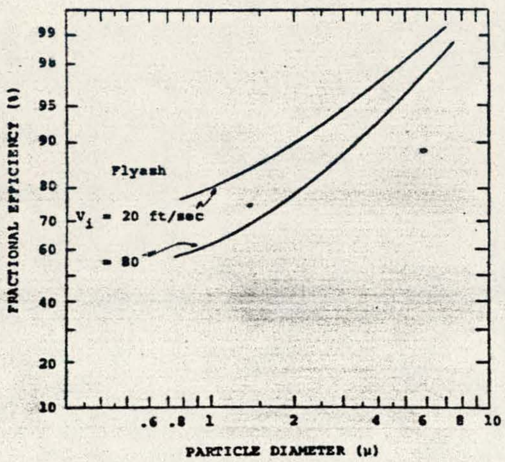

FIGURE 14: THEORETICAL CORRELATION OF ELECTROSTATIC AUGMENTATION WITH FLYASH

Comparative Performance

Figure 15 compares the test results of the present work with previous work. All data is without electrostatic augmentation. As previously noted, the 18 in. diameter electrocyclone model is a derivative of the Stairmand High Efficiency design (with low flow handling capacity, $Q = 0.1D^2V_i$) while the earlier 12 in. diameter air shield model is a derivative of the Stairmand High Flow design ($Q=0.281D^2V_i$). Hence, the reported data is shown for reference. The reported data for the high flow design appears to be unduly pessimistic. Tests of an approximate model were found to yield much higher efficiency of collection (13). The earlier air shield cyclone, both with and without the clean air shielding feature, was found to embody design features significantly superior to the basic Stairmand design. These are presumed to include a longer engagement length (between the exhaust and the cyclone body) and a smaller exhaust diameter (increased spin-up). The present model data in this comparison is found to provide only a slight additional improvement in spite of the much higher spin-up provided by the smaller exhaust. It is concluded that an additional design feature is penalizing the present design.

Table 1 summarizes the basic design features of different cyclones, exclusive of the air shielding feature.

Particular attention may be drawn to the ratio of flow area at the cyclone annulus versus inlet. It is noted that excessive flow diffusion exists with the High Efficiency configuration. This would be expected to result in excessive flow separation and turbulent mixing at the cyclone inlet. This situation is also evident in the High Flow design, but to a much lesser extent. A preferred design would provide for an accelerating inlet flow turn (or the use of axial swirl vanes) as indicated for a recommended design shown in Figure 16. The ideal design is intended to suggest preferred trends.

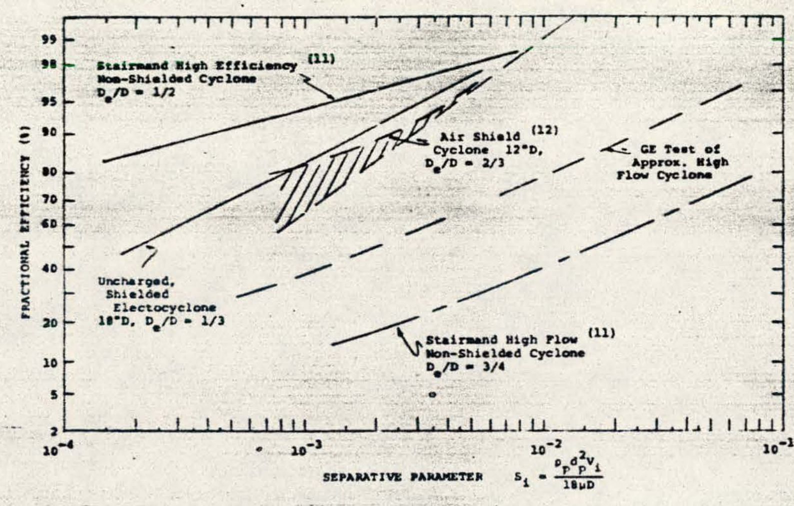

FIGURE 15: COMPARATIVE CYCLONE PERFORMANCE DATA

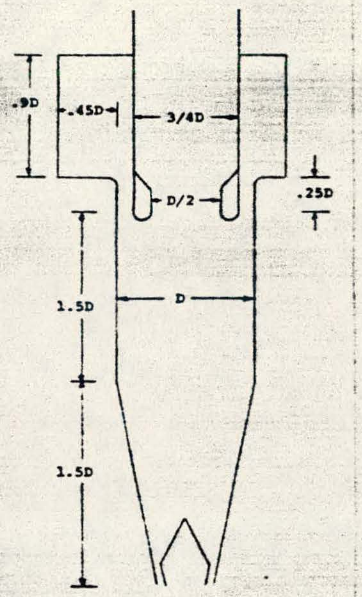

FIGURE 16: BASIC RECOMMENDED DESIGN

Summary

These cold flow investigations show an electrostatic enhancement particularly for fine dusts which are projected to be especially beneficial for large cyclones. Present data suggests, however, that performance is inhibited for dense dusts and at high velocity. It is hypothesized that the main problem is due to an inlet flow maldistribution associated with the use of small inlets, typical of high performance cyclones.

Acknowledgement

This work was performed under sponsorship of the U.S. Department of Energy, Contract No. DE-AC01-80ET17091.

References

1. Giles, W.B. "Electrostatic Separation in Cyclones" Symposium on the Transfer and Utilization of Particulate Control Technology, Vol. III, Sect. B., p. 291-302, Feb., 1979.

TABLE 1
BASIC CYCLONE DESIGN PARAMETER COMPARISON
(Body Diameter = D)

	Stairmand High Efficiency	Stairmand High Flow	Basic Air Shield	Recommended	R&D Ideal
Inlet Type	Tangential	Scroll	Scroll	Scroll	Annular Turn
Inlet, x/D	0.5 x 0.2	0.75 x 0.375	0.75 x 0.375	0.9 x 0.45	0.9 x 0.45
Overall Length, L/D	4	4	3	4.15	≈ 6
Dust Exit, De/D	3/8, Dump	3/8, Dump	3/8, V.S.*	3/8, V.S.*	3/8, V.S.*
Inlet Area/D^2	0.10	0.2813	0.2813	0.405	0.405
Annulus Area/D^2	0.589	0.3434	0.3434	0.3434	<0.3434
Outlet, D_e/D	0.5	0.75	0.67	0.5(Dif.)**	<0.5(Dif.)**
Outlet Area/D^2	0.1963	0.4416	0.3489	0.1963	<0.1963
Inlet Vol./D^3	0.2944	0.783	0.783	0.663	>0.663
Body Vol./D^3	1.776	1.482	1.085	1.772	≈3.225
Spin-up Ratio	2.8	2.33	2.63	3.90	>3.90
Engagement Length/D***	0	1/8	1/8	1/4	>1/4

* Vortex Shield

** Diffuser

*** Axial Length Between Inlet and Exhaust

2. Petroll, J. & Langhammer, K., "Comparative Tests on Cyclone Precipitators," Breiberger Forschungsheft, Vol. A220, pp. 175-196, 1962.

3. Ludewig, H., "Cyclone Model Experiments Regarding the Effect of the Dip Pipe Depth on Separating Efficiency and Pressure Drop," Vol. 7, No. 8, pp. 416-421, 1958.

4. ter Linden, A.J., "Investigations in Cyclone Separators," VDI Seminar, Vol. 3, 1954, VDI Verlag.

5. Berth, W. & Trunzk, "Model Test with Water Stream Cyclone Separator for Predetermining Removal Efficiency," Z.F. Angew, Mat and Mech., Vol. 30, 1950, No. 8/9.

6. Rammler, E. and Breitling, K., "Comparative Tests with Centrifugal Separators,"Freiberger Forschungsheft, A56, 1957.

7. Verbal communication with Weber and Klein of Siemens Kraftwork Union.

8. Reif, R., U.S. Patent 4,010,011, March 1, 1977.

9. Hodson, P., U.S. Patent 2,748,880, June 5, 1956.

10. Rommel, W.R., U.S. Patent 2,594,805, June 26, 1945.

11. Stairmand, C.J."Design and Performance of Cyclone Separators" Trans. Instn. Chem. Engr's., Vol. 29, 1951, p. 356-383.

12. Anomy. "PBG-CFCC Development Program-Adv. Cleanup Device Performance Design Report (Task 4.3) Vol. B-Air Shield Cyclone Evaluation", Prep. for U.S. DoE Contract No. EX-76-C-01-2357, Dist. Category UC-90e, FE-2357-70.

13. Bekofske, K.L. "Air Shield Cyclone in Non-Shielded Configuration", Letter report dated 1/24/80.

Nomenclature

A_i	= cyclone inlet area	E	= electric field
d_p	= particle diameter	F_d	= drag force
$d_{p50} \equiv d_p$	= particle mass mean dia.	F_e	= electrostatic force
D	= cyclone diameter	F_i	= inertial force
D_e	= exhaust diameter	L	= length
D_{el}	= electrode diameter	Δ_p	= differential pressure

p = penetration - $1-\eta_f$

Q = cyclone flow

q_p = particle charge

r = radius

S = separative parameter

S_i = inertial separating parameter

U_r = radial velocity at r

V_i = cyclone inlet velocity

V_t = cyclone tangential velocity

V_o = voltage differential

x = inlet scroll width

Greek

η = overall cyclone efficiency

η_f = fractional efficiency

ρ = gas density

ρ_r = particle density

μ = absolute gas viscosity

ε = permittivity of air